An Experimental Raman and Theoretical DFT Study on the Self-Association of Acrylonitrile

Jose M. Alía,*,† Howell G. M. Edwards,‡ W. Ronald Fawcett,† and Thomas G. Smagala†

Department of Chemistry, University of California, Davis, California 95616, and Chemical and Forensic Sciences, School of Pharmacy, University of Bradford, Bradford, BD7 1DP, United Kingdom

Received: September 26, 2006; In Final Form: November 24, 2006

The liquid structure of acrylonitrile (propenenitrile) has been investigated using Raman spectroscopy and density functional theory (DFT) ab initio calculations with the 6-311++G** basis set. Two different and complementary experimental approaches were undertaken: FT−Raman spectra of 13 acrylonitrile solutions in carbon tetrachloride (concentration range = 0.25−12.0 mol·L^{-1}) were studied in detail including principal component analysis (PCA) of the C≡N stretching band. Furthermore, dispersive Raman spectra of neat acrylonitrile were obtained at eight different temperatures from 238 up to 343 K. The complex and asymmetric acrylonitrile Raman C≡N stretching band can be decomposed into two components attributed to monomeric and self-associated forms. Ab initio results fully support this assignment and suggest that the self-associated complex is a nonplanar trimer held together by dipole−dipole interactions. At ambient temperature, the composition of acrylonitrile can be expressed as a mixture of 25% monomers and 75% trimers. Close to the boiling point, trimers still represent 65% of the liquid composition. The corresponding enthalpy of association was estimated to be -22 ± 2 kJ·mol^{-1}.

1. Introduction

Self-association in nitriles has been well-documented. Macroscopic measurements (dielectric constants,[1] dielectric polarization,[2] excess volumes[3]), thermodynamic calculations,[4] nuclear magnetic resonance,[5−7] mass spectrometry,[8,9] and vibrational spectroscopy (infrared and Raman)[10−18] have confirmed that intermolecular associations, through dipole/dipole interactions, are strong in nitriles. This follows from the electronic structure of the C≡N functional group. On the other hand, numerous theoretical approaches support the particular stability of nitrile aggregates consisting of dimers, trimers, and even higher molecular clusters.[13,19−27] There are, however, several questions still unresolved. First of all, the possibility of self-association through a hydrogen bond between the nitrogen lone pair and one alpha hydrogen of a neighbor molecule, as several ab initio[15,24−26] and mass spectrometry[9] studies suggest, has not been spectroscopically studied. Even though it is clear that the main driving force to promote self-association in nitriles must be its strong dipolar character, hydrogen bonding may further contribute to stabilize the associated system. Moreover, from the vibrational point of view, the complete explanation of the asymmetric shape generally observed in the infrared and Raman C≡N stretching band of many nitriles[28−32] is still controversial. In 1973, Griffiths[33] observed this feature in the Raman spectrum of liquid acetonitrile and analyzed the band contour through band-fitting techniques, decomposing it into two components. He attributed these sub-bands to acetonitrile monomers (narrower component located at higher wavenumbers) and aggregates (broader component at lower wavenumbers) and suggested an equilibrium between both species. Shortly thereafter, Loewenschuss and Yellin[34] showed that the secondary structure of the ν(C≡N) band seems to be insensitive to dilution in inert solvents and to temperature changes; thus, they concluded that there is no specific equilibrium between different chemical aggregates. Instead, liquid acetonitrile would have a cluster structure with molecules located in two different environments (in the clusters' periphery and inside the clusters) giving rise to two separated vibrational signals. On the other hand, several authors have justified the complex band structure of this acetonitrile fundamental as because of Fermi resonance with the combination band $\nu_3 + \nu_4$ (CH_3 deformation and C−C stretching bands)[35,36] or by the presence of hot band transitions from the first excited state of the degenerate C−C≡N bending ν_8 mode.[37−39] These problems, inherent in the complex vibrational behavior of acetonitrile, could be avoided by using acrylonitrile, which is simpler from a spectroscopic point of view. Furthermore, because of its low symmetry, it has no degenerate vibrations. The combination of CH_2 deformation and C−C stretching bands (ν_6 and ν_9 in acrylonitrile) appears at 2281.3 cm^{-1}, far enough from the ν(C≡N) fundamental (2229.6 cm^{-1}), so that it does not enter into resonance.[40] We have published a series of studies on electrolyte solutions in acrylonitrile using vibrational spectroscopy,[41−51] and its behavior is similar to that observed in acetonitrile[52] and other nitriles such as benzonitrile[53,54] or propionitrile.[55−57]

A detailed FT−Raman study of 13 solutions of acrylonitrile in CCl_4 is presented here with the aim to clarify the existence of a true equilibrium between definite chemical species in nitriles. Evolution of the C≡N stretching band position and shape is monitored up to concentrations of 0.25 mol·L^{-1} (acrylonitrile mole fraction = 0.024). The system is also modeled using density functional theory (DFT) ab initio calculations, with consideration given to dimer and three

* To whom correspondence should be addressed. E-mail: josemaria.alia@uclm.es. Permanent address: Universidad de Castilla-La Mancha, Dpto. de Química Física, E.U.I.T.A., Ronda de Calatrava 7, 13071 Ciudad Real, Spain.

† University of California.

‡ University of Bradford.

10.1021/jp0663210 CCC: $37.00
Published on Web 01/17/2007

TABLE 1: Characteristics of the Studied Solutions[a]

g ACN	g CCl_4	density	[ACN]	[CCl_4]	χ ACN
0.0666	7.7038	1.5541	0.25	10.02	0.024
0.1421	7.5500	1.5384	0.54	9.82	0.052
0.2714	7.3093	1.5161	1.02	9.50	0.097
0.5322	6.8275	1.4719	2.01	8.88	0.184
0.8020	6.2735	1.4151	3.02	8.16	0.270
1.0773	5.7934	1.3741	4.06	7.53	0.350
1.3345	5.2362	1.3141	5.03	6.81	0.425
1.6055	4.7090	1.2629	6.05	6.12	0.497
1.8709	4.1890	1.2198	7.05	5.45	0.564
2.1239	3.6844	1.1617	8.01	4.79	0.626
2.4031	3.1382	1.1083	9.06	4.08	0.689
2.6516	2.6391	1.0581	9.99	3.43	0.744
3.1911	1.5269	0.9436	12.03	1.99	0.858

[a] ACN = acrylonitrile. Densities are given in units of kg·L^{-1} and concentrations are given in mol·L^{-1}. χ = mole fraction.

different trimers. Finally, a dispersive Raman study of neat acrylonitrile at different temperatures from 238 up to 343 K is carried out.

2. Experimental

2.1. Reagents and Solutions. Acrylonitrile and carbon tetrachloride (Aldrich) of the best available quality were used as received. IR spectroscopy did not reveal the presence of any significant amount of water. Thirteen solutions, whose characteristics are given in Table 1, were prepared by weight and their densities at 20 °C were measured in a conventional picnometer. Raman spectra were always recorded from freshly prepared solutions filtered through 0.65-μm Millipore filters.

2.2. FT−Raman Spectra. FT−Raman spectra were excited at 1064 nm using an Nd:YAG laser and a Bruker IFS66 optical bench with an FRA 106 Raman accessory. Laser power was set at 100−110 mW, and 2000 scans were accumulated with a resolution of 2 cm^{-1}. The temperature was 20 ± 1 °C. The integral intensities of the CCl_4 Raman bands at 461 and 315 cm^{-1} were used as internal standards to normalize the different spectra.

2.3. Computational Details. The starting structure for acrylonitrile was taken from the literature.[58] Initial structures of planar dimer and trimer (trimer I) and cyclic trimer (trimer III) were constructed from the optimized structure of acrylonitrile, locating the monomers at similar intermolecular distances to those published for acetonitrile complexes.[23] For the nonplanar trimer (trimer II), the starting structure was that of Katayama et al.[59] Becke's gradient-corrected exchange functional[60] in conjunction with the Lee−Yang−Parr correlation functional[61] with three parameters (B3LYP)[62] was used for all calculations. The employed basis set (6-311++G**) seems to be particularly suitable to obtain reliable vibrational parameters.[63−66] All of the DFT-optimized structures were in a minimum of the potential energy surface as can be inferred from the absence of negative (imaginary) frequencies. The Born−Oppenheimer total energies, zero-point vibrational energies (calculated within the harmonic approximation), and the thermal enthalpies at 298 K were calculated using the unscaled harmonic vibrational frequencies. The effect of the basis-set superposition error (BSSE) was analyzed in the optimized structure of the complexes by the standard counterpoise method.[67,68] As usual, the complex binding energy is defined as

$$\Delta E = [E_{\text{complex}} - n(E_{\text{acrylonitrile}})] + E_{\text{BSSE}} \qquad (1)$$

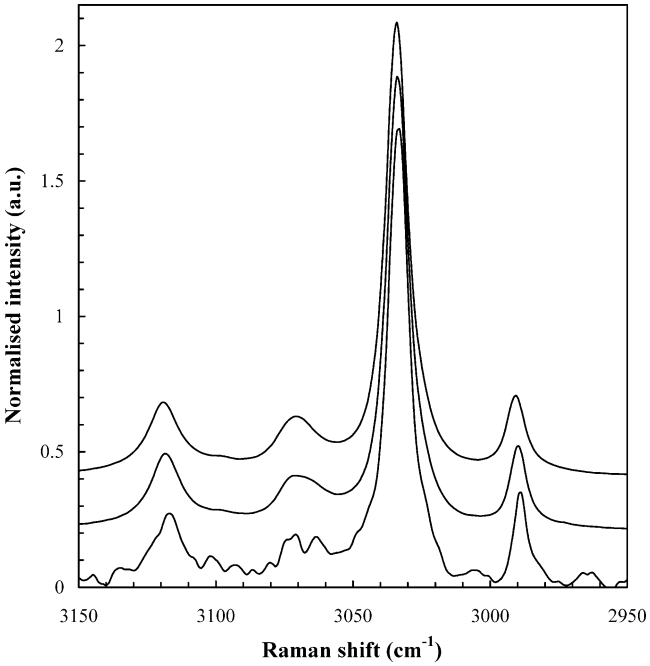

Figure 1. Raman C−H stretching region in neat acrylonitrile (top), 6.0 mol·L^{-1} (middle), and 1.0 mol·L-1 (bottom) in CCl_4.

where n is the number of monomers (2 or 3) considered and

$$E_i = E_{\text{electronic}} + E_{\text{ZPE}} \qquad (i = \text{complex or acrylonitrile}) \qquad (2)$$

All these calculations were carried out with the Gaussian 03 program package[69] in the Supercomputation Centre of the Universidad de Castilla-La Mancha, which uses HP AlphaServer GS80 and Silicon Graphics Origin 2000 workstations. The Ampac GUI 8 system[70] was the graphic interface that facilitated the study of the vibrational modes. Statistical procedures such as principal component analysis (PCA) and curve fitting were run with the application STATGRAPHICS+ (5.1) for Windows.[71]

2.4. Dispersive Raman Spectra. Raman excitation was accomplished with a Spectra-Physics 2020/5 argon ion laser operating at 488.0 nm, with a power of 800 mW. The scattered radiation was analyzed using a SPEX 1401 Czerny-Turner 0.85-m spectrometer with a spectral slit-width of 4 cm^{-1}. Photon-counting detection was carried out with an EM1 9787 QA photomultiplier. Acquisition of the data and control of the spectrometer were accomplished using a Thorn EMI-PET microcomputer. Calibration was effected using a neon emission spectrum, and wavenumbers are correct to within 1 cm^{-1}. For all Raman spectroscopic measurements, the solutions of interest were held in an evacuated double-jacketed glass cell. The cell temperature was controlled by industrial alcohol circulation (Julabo F40HC circulatory system) to within 0.5 K over the temperature range studied, namely, 238−343 K. The scans were acquired with a speed of 50 cm^{-1} min^{-1} using an accumulation of 10 scans per spectrum and a spectral density of 2 data points per cm^{-1}.

Dispersive Raman data files and original FT-Raman spectral data in OPUS (Bruker) format were converted to JCAMP format and were processed with the commercial software GRAMS/32 AI (6.00) (Galactic Industries). This package fits the peaks using mixed Gaussian−Lorentzian linear combinations

$$f(\nu) = (1 - M)\cdot(\text{Gauss}) + M\cdot(\text{Lorentz}) \qquad (3)$$

where M is the fraction of Lorentzian shape.

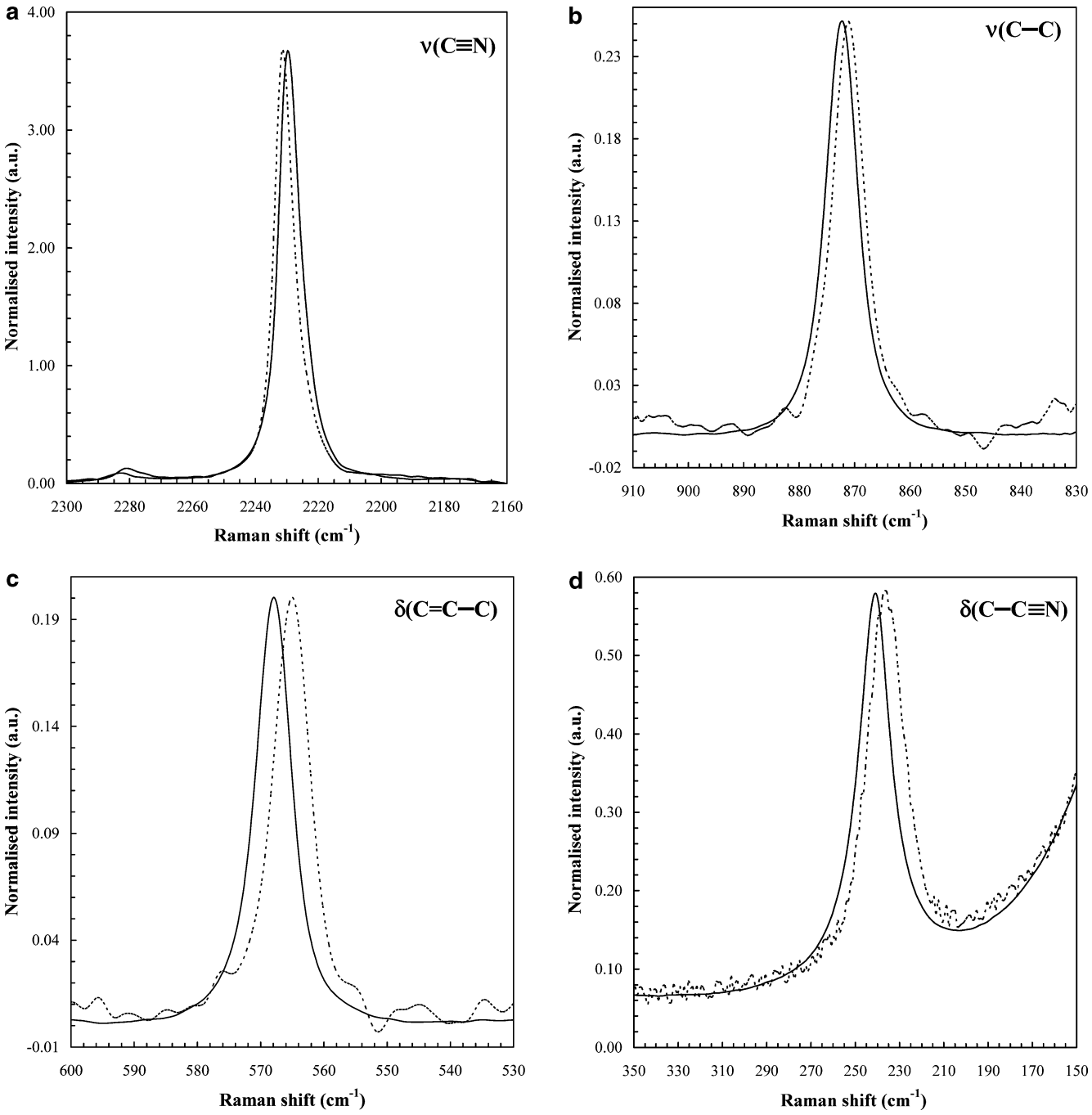

Figure 2. Four Raman spectral regions in neat acrylonitrile (full line) and 1.0 mol·L^{-1} (dotted line) in CCl_4.

3. Results and Discussion

3.1. FT-Raman Spectroscopy. As was previously mentioned, the possibility of hydrogen bonding between the nitrile nitrogen lone pair and one alpha hydrogen of a vicinal molecule could justify the well-documented self-association of nitriles. Figure 1 shows the Raman C−H stretching region in three samples: neat acrylonitrile and 6.0 and 1.0 M solutions in CCl_4. The lack of any spectral change in wavenumber and bandwidth allows one to rule out this kind of molecular interaction in the case of acrylonitrile. Indeed, band maxima maintain their frequencies despite the dilution and there is no band broadening, which are two sine qua non factors to spectroscopically confirm the presence of hydrogen bonding,[72−74] proper (conventional) or improper (blue-shifting).[75]

Figure 2 shows the main spectral modifications observed in the acrylonitrile fundamentals when it dissolves in CCl_4. The bands shift slightly toward lower wavenumbers except in C≡N stretching where the behavior is the opposite. Figure 3 shows the wavenumbers of the corresponding maxima against the mole fraction of acrylonitrile. The observed red-shifts vary between −1.2 cm^{-1} for the C−C stretch and −6.4 cm^{-1} for the C−C≡N out-of-plane bending mode. The remaining vibrations are affected by the dilution in the same way. Specifically, only the C≡N stretching is blue-shifted by +2.2 cm^{-1}. Similar trends have been reported in other nitriles[76] such as acetonitrile and benzonitrile dissolved in carbon tetrachloride,[17,32] benzene,[31] DMF, and DMSO.[16] However, these band shifts are not accompanied by changes in bandwidth with the exception of the most diluted solutions at concentrations of 0.25 and 0.50 mol·L^{-1}. In those solutions, narrowing is observed in the C≡N stretching region, in agreement with previous reports.[10] Figure 2 also illustrates that ν(C≡N) band is asymmetric, favoring

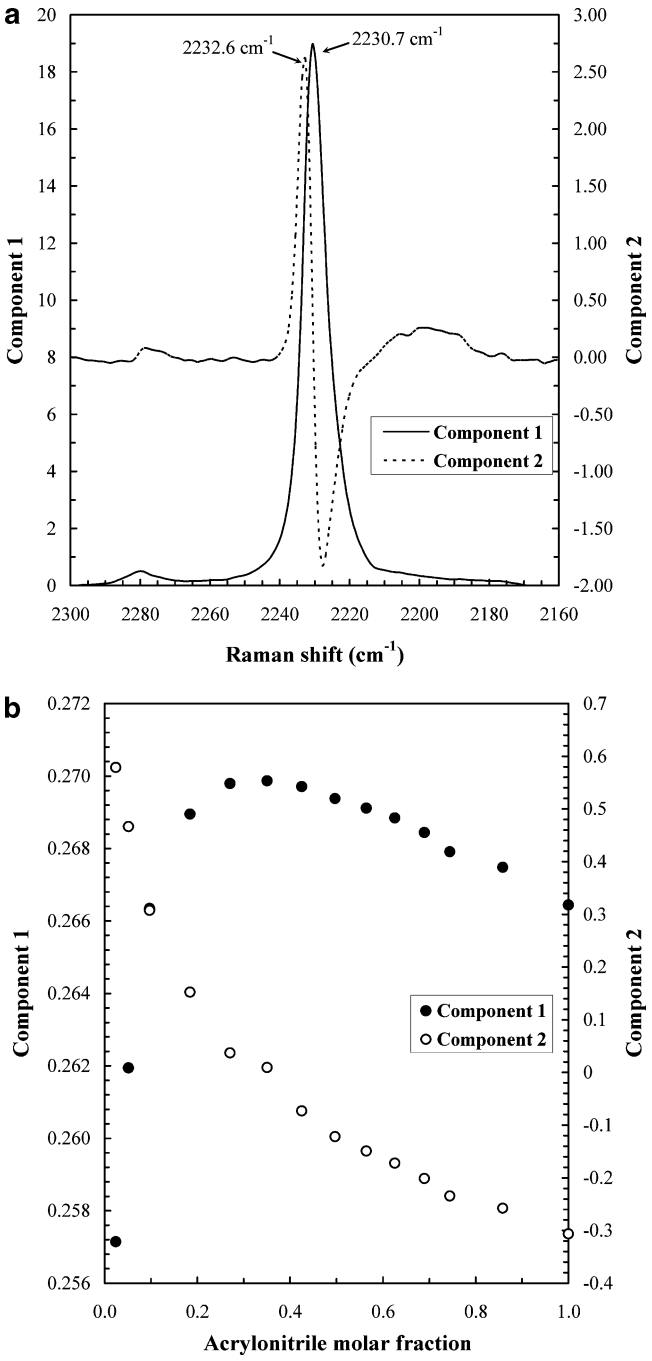

Figure 3. Results of the principal component analysis (PCA) in the ν(C≡N) Raman spectral region of acrylonitrile dissolved in CCl_4. (a) Significant principal components. (b) Components weight against the corresponding molar fractions of acrylonitrile.

lower frequencies. The asymmetry of this band is characteristic of several nitriles[17,18,28,30,77] and, in the case of acrylonitrile, seems to remain even in Ar matrixes at 12 K.[77] Various other possible explanations exist for justifying this characteristic asymmetry, such as the presence of hot bands in the vibrational spectrum of acetonitrile.[37,39] The cluster structure of liquid nitriles should permit single molecules to be in two different environments, periphery and interior of the cluster, and thus results in two separated vibrational signals.[34] However, it is generally accepted[15,17,28,33,53,78] that the asymmetry could arise from the simultaneous presence of monomers and higher aggregates. Furthermore, as we have previously reported,[79] the simultaneous presence of both hot bands and new bands attributable to associated acetonitrile is also possible. Nevertheless, there appears to be no evidence in the literature attempting to quantify the probable aggregation equilibrium with the exception of a report from Perelygin et al.[80] regarding acetonitrile dissolved in carbon tetrachloride. Band-component fitting is readily achieved when the different components are sufficiently separated to produce well-differentiated signals. However, when components are so overlapped that asymmetry occurs in a band, the task is not so obvious, as in the present case. Thus, some preliminary objective information is advisable to avoid any a priori or arbitrary presumption.

TABLE 2: Results of the Principal Component Analysis: Eigenvalues (EV), Explained Variance (%), and Successive Eigenvalues Quotient, $EV_{(i+1)}/EV_{(i)}$

component no.	eigenvalue	explained variance (%)	cumulative (%)	$EV_{(i+1)}/EV_{(i)}$
1	1.2725E+01	97.887	97.887	46.84
2	2.7165E-01	2.090	99.977	114.63
3	2.3699E-03	0.018	99.995	4.79
4	4.9518E-04	0.004	99.999	7.52
5	6.5848E-05	0.001	99.999	1.54
6	4.2685E-05	0.000	100.000	1.13
7	3.7757E-05	0.000	100.000	8.30
8	4.5463E-06	0.000	100.000	1.80
9	2.5298E-06	0.000	100.000	3.40
10	7.4334E-07	0.000	100.000	1.12
11	6.6088E-07	0.000	100.000	1.79
12	3.6914E-07	0.000	100.000	2.34
13	1.5766E-07	0.000	100.000	

To gain some information about the number of components and its corresponding wavenumbers, a statistical PCA was undertaken. PCA is a useful tool that allows one to identify the number of components in a complex envelope band[81−83] and has proven to be successful in the analysis of complicated vibrational bands.[47,84−87] The statistical analysis was done for spectra of acrylonitrile solutions in CCl_4 at 13 different concentrations (see Table 1), with 146 experimental intensity points per spectrum. This corresponds to the 2190−2267 cm^{-1} Raman spectral region where the ν(C≡N) band appears. Thus, a matrix of 13 × 84 was computed and its 13 eigenvalues are given in Table 2. The number of statistically significant eigenvalues will give the number of components in the complex band. There are several methods to obtain this number[80,81] that usually imply the previous knowledge of the exact error in the experimental data. However, it is easier and more practical to calculate the quotients between two successive eigenvalues, that is,

$$\text{quotient} = \frac{EV_{(i+1)}}{EV_{(i)}} \tag{4}$$

and consider only those eigenvalues whose quotients are different from the rest.[83] In this case (see Table 2), this implies that only two components explain the complex band. The corresponding eigenvectors are represented in Figure 3a. The chemical meaning of these eigenvectors, which are linear combinations of the experimental spectra multiplied by their corresponding weights, is quite simple. The first component reproduces an averaged experimental spectrum, while the second one represents the averaged effect of the perturbing agent (in this case, the presence of CCl_4) over the spectra. The CCl_4 promotes the raising of spectral intensity in the higher wavenumber side (maximum: 2232.6 cm^{-1}) and the corresponding decrease in the lower wavenumber side (minimum: 2227.8 cm^{-1}). The calculated weights for the different samples are also plotted in Figure 3b. Note how the weights corresponding to the first eigenvector, principal component 1, change moderately

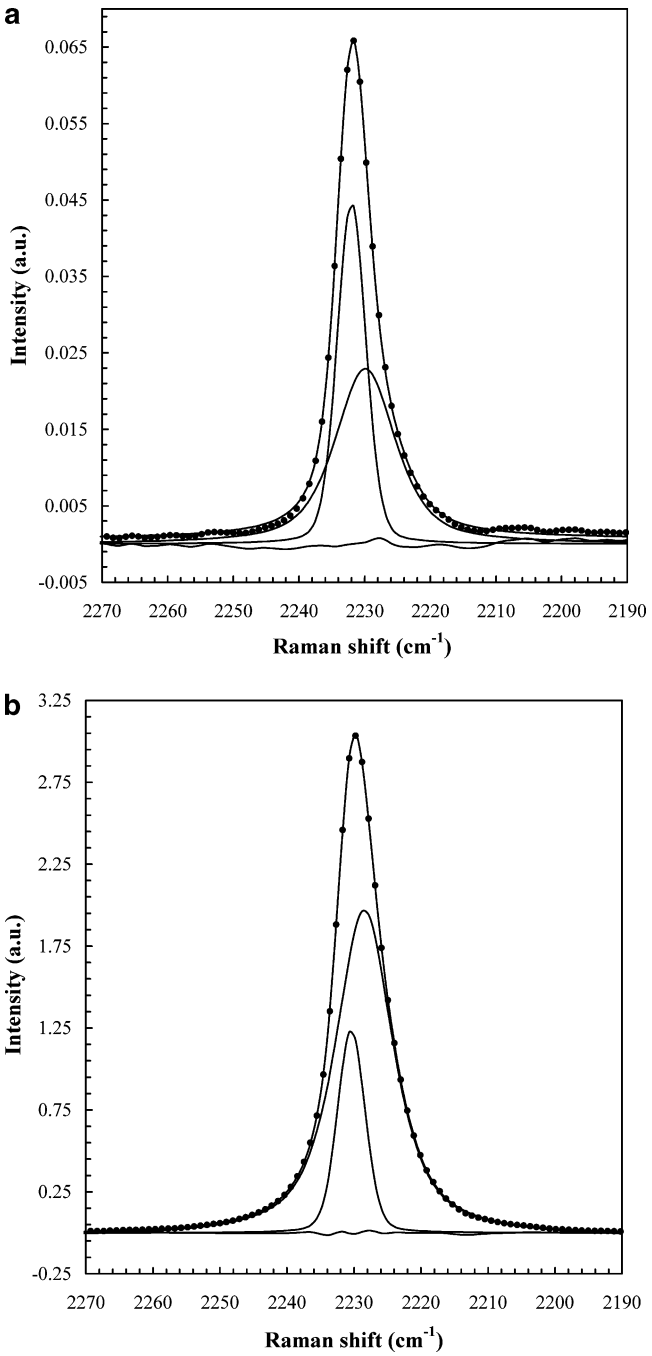

Figure 4. Results (experimental spectrum, fitted spectrum, components, and residual) of the band-fitting procedure in the ν(C≡N) complex band. (a) Acrylonitrile, 0.25 mol·L^{-1} in CCl_4. (b) Neat acrylonitrile. Points: experimental spectrum.

(range: 0.2658−0.2803), but those corresponding to the second eigenvector, principal component 2, vary considerably, with values that decrease when the acrylonitrile concentration increases. This implies that the effect of the perturbing agent is a direct function of its relative concentration. Thus, the effect of the dilution in carbon tetrachloride is to promote the presence of the species whose ν(C≡N) Raman band is located at higher wavenumbers. As will be demonstrated later via ab initio calculations, this species is the acrylonitrile monomer. Furthermore, the split between the ν(C≡N) Raman bands from the monomer and the associated acrylonitrile must be in the vicinity of 1.9 cm^{-1} which is the difference between the wavenumbers corresponding to both maxima, as can be observed in Figure 3b. Thus, band-fitting procedures must demonstrate the presence of two components, separated by an average of 1.9 cm^{-1} and located close to 2232 and 2230 cm^{-1}. These should correspond to the free (monomer) and associated (oligomer) acrylonitrile. Clearly, the concentration of the free form must increase with the dilution in CCl_4.

With these initial calculations, band-fitting was undertaken in the same spectral portion (2160−2300 cm^{-1}) in which the PCA was done. The results are shown in Figure 4 and Table 3. During the band-fitting procedure, no parameters (band position, full width at half-height or Lorentzian character) were fixed, allowing the program to find the most appropriate set to reach convergence in its search for the two bands. As shown in Table 3, the band attributed to free (monomer) acrylonitrile is narrower than the one corresponding to the associated (oligomer) acrylonitrile. Furthermore, its shape is more Gaussian and corresponds to a chemical species with lower vibrational relaxation times than the associated acrylonitrile.[30,32,88] The narrowing of the C≡N stretching band when a nitrile is dissolved in CCl_4 has been previously documented in several cases.[10] This could be explained as a direct structure-breaking effect of the solvent over the nitrile self-associated structure. The splitting between the calculated components is 2.13 ± 0.15 cm^{-1}, which is in excellent agreement with the PCA result which predicts a separation of 1.9 cm^{-1}. Once the relative intensities (areas) of both species have been obtained, the corresponding Raman molar intensity coefficients (J) can be computed. For this purpose, the method proposed by Shurvell and co-workers[55−57] is used, which has been applied to different electrolyte and organic acid solutions in nonaqueous solvents.[51,89,90] In this method, C_T is the total molar concentration of acrylonitrile (ACN) in CCl_4, C_F is the molar concentration of the free (monomer), and C_A is the molar concentration of the associated (oligomer)

$$C_T = C_F + C_A \tag{5}$$

For each species, the intensity/concentration relationship must hold

$$I_i = J_i C_i \tag{6}$$

where I_i are the integrated band intensities, J_i is the molar Raman scattering factors, and C_i is the molar concentration of each species. Combining eqs 5 and 6

$$C_T = \frac{I_F}{J_F} + \frac{I_A}{J_A} \tag{7}$$

and eq 7 can then be rearranged to yield

$$\frac{I_A}{C_T} = J_A - \frac{J_A I_F}{J_F C_T} \tag{8}$$

A plot of I_A/C_T against I_F/C_T should give a straight line with an intercept equal to J_A and a slope equal to $-J_A/J_F$. Such a plot is shown in Figure 5. From the intercept and the slope, it was found that J_A = 3.2713 ± 0.0573 and J_F = 2.0945 ± 0.1425. The Raman molar scattering coefficient significantly decreases in the monomeric form of acrylonitrile (36%). The same appears to occur with the infrared molar absorption coefficient, which decreases on average when nitriles are dissolved in nonpolar aprotic solvents.[10] Once the molar scattering coefficients have been obtained, the corresponding molar concentrations of free (monomer) and associated (oligomer) ACN can be calculated. Table 4 shows the numerical

TABLE 3: Pure Acrylonitrile and Acrylonitrile Solutions in CCl_4, Band-Fitting Results in the C≡N Stretching Raman Band Contour[a]

	free nitrile				associated nitrile			
[ACN]	center	fwhh	Lorentz (%)	area	center	fwhh	Lorentz (%)	area
0.25	2232.0	5.15	19.6	0.2559	2229.9	10.96	61.1	0.4060
0.54	2231.8	5.33	23.3	0.5788	2229.5	11.40	65.1	0.8843
1.02	2231.5	5.24	21.4	0.9793	2229.2	11.80	62.6	1.7586
2.01	2231.2	5.15	22.3	1.7627	2228.9	11.64	63.4	3.8327
3.02	2231.0	5.11	22.0	2.4725	2228.7	11.42	63.9	6.0406
4.06	2231.0	5.08	22.9	3.1082	2228.8	11.18	63.7	8.4038
5.03	2230.8	5.03	23.7	3.6276	2228.6	11.04	66.0	10.7108
6.05	2230.7	4.99	25.6	4.2510	2228.5	10.93	67.0	13.4341
7.05	2230.6	4.99	25.0	4.7882	2228.5	10.89	67.3	15.7492
8.01	2230.6	4.96	26.3	5.1665	2228.5	10.80	68.5	17.8972
9.06	2230.5	4.98	26.9	5.7451	2228.5	10.46	68.7	20.8211
9.99	2230.4	4.94	26.6	6.1792	2228.5	10.38	69.9	23.5638
12.03	2230.4	4.86	29.8	6.9565	2228.5	10.28	73.0	28.7318
14.93 (neat)	2230.3	4.76	33.7	7.7772	2228.4	10.11	77.2	35.5628

[a] [ACN] in units of mol·L^{-1}; centers and full width at half-height (fwhh), cm^{-1}; areas, arbitrary units × cm^{-1}.

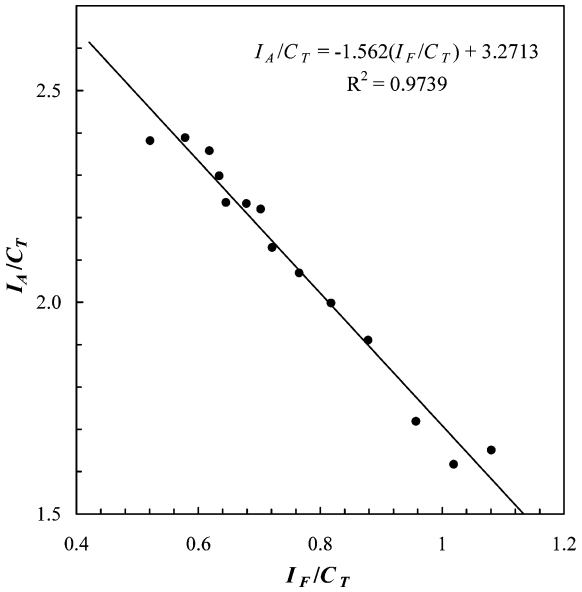

Figure 5. Shurvell and co-workers' plot[55−57] corresponding to the solutions of acrylonitrile in CCl_4.

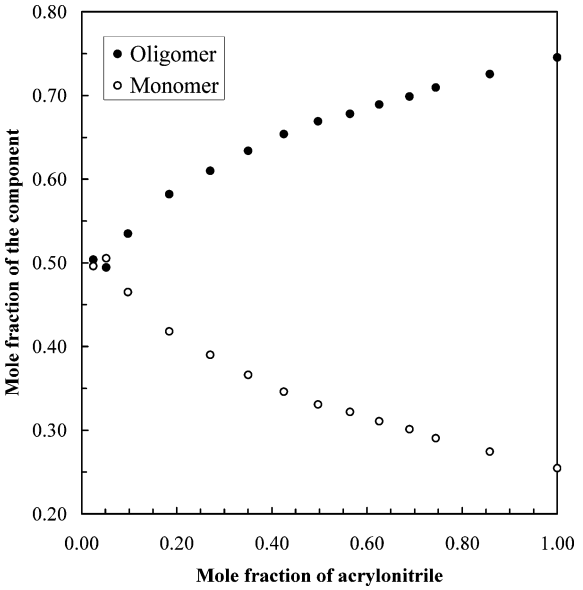

Figure 6. Calculated mole fractions of free (monomer) and associated (oligomer) acrylonitrile against the mole fraction of acrylonitrile in CCl_4.

TABLE 4: Calculated Molar Concentrations and Mole Fractions of Free (Monomer) and Associated (Oligomer) Acrylonitrile in CCl_4 Solutions

C_F	C_A	calculated C_T	nominal C_T	χ_F	χ_A
0.12	0.12	0.25	0.25	0.4960	0.5040
0.28	0.27	0.55	0.54	0.5055	0.4945
0.47	0.54	1.01	1.02	0.4652	0.5348
0.84	1.17	2.01	2.01	0.4180	0.5820
1.18	1.85	3.03	3.02	0.3900	0.6100
1.48	2.57	4.05	4.06	0.3661	0.6339
1.73	3.27	5.01	5.03	0.3460	0.6540
2.03	4.11	6.14	6.05	0.3308	0.6692
2.29	4.81	7.10	7.05	0.3220	0.6780
2.47	5.47	7.94	8.01	0.3108	0.6892
2.74	6.36	9.11	9.06	0.3012	0.6988
2.95	7.20	10.15	9.99	0.2906	0.7094
3.32	8.78	12.10	12.03	0.2744	0.7256
3.71	10.87	14.58	14.93	0.2546	0.7454

results of these calculations. The differences between the calculated total ACN concentration and the nominal concentration of the solvent are within the experimental error (mean quadratic error = 0.1096). When molar concentration data are converted to mole fractions for both acrylonitrile species, the data presented in Figure 6 are obtained. It is important to emphasize that in neat acrylonitrile, the mole fraction of free (monomer) molecules should be approximately 0.25, in good agreement with values previously calculated[1] or estimated[4] using nonspectroscopic measurements. Until now, the associated form of acrylonitrile has been designated as an oligomer, without any presumption about its stoichiometry or structure. This occurs because Raman spectroscopy fails to provide this information in the studied range of wavenumbers ($\nu > 100$ cm^{-1}). Thus, the corresponding constant for the self-association equilibrium cannot be computed. To account for the presence of self-associated forms of acrylonitrile in liquid state and to discuss their structure on the basis of their vibrational spectra, we have carried out ab initio quantum calculations. Those results are presented and discussed in the next section.

3.2. Ab Initio Calculations. Optimized structures of acrylonitrile dimer, planar trimer (trimer I), nonplanar trimer (trimer II), and cyclic trimer (trimer III) are given in Figure 7. As in other reported nitriles, the planar trimer is simply a dimer in which a third monomer molecule is added in an antiparallel manner.[23,24,91] Trimer II has a considerably different configuration in which two parallel molecules simultaneously coordinate

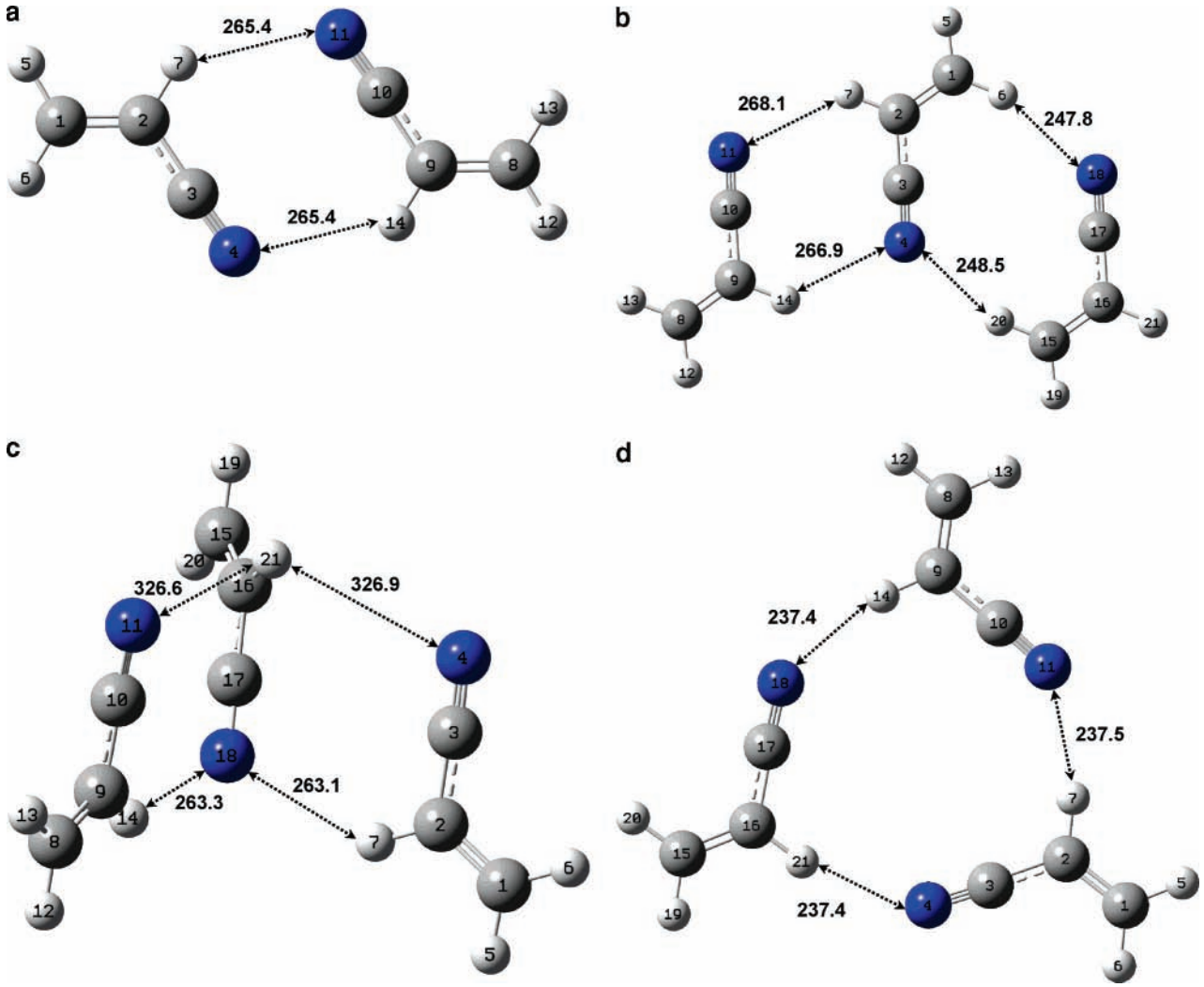

Figure 7. DFT optimized structure of acrylonitrile aggregates (a) dimer, (b) trimer I, (c) trimer II, and (d) trimer III. Level of theory: B3LYP/6-311++G**. Distances (in pm) represent closest approaches, not hydrogen bond lengths.

TABLE 5: Optimized Structural Parameters, Calculated Dipole Moments, and ΔE (kJ mol^{-1}) of the Studied Acrylonitrile Species at the B3LYP/6-311++G Level of Theory[d]**

parameter	experimental[a]	experimental[b]	monomer	dimer	trimer I	trimer II	trimer III
C═C	133.9	134.3	133.5	133.5	133.6	133.5	133.6
C−C	142.6	143.8	142.8	142.8	142.8	142.7	142.8
C≡N	116.4	116.7	115.6	115.6	115.6	115.6	115.6
CH (in CH_2)	108.6	111.4	108.3	108.3	108.4	108.3	108.4
CH (in ═CH)			108.5	108.6	108.6	108.4	108.7
∠CCC	122.6	121.7	123.1	122.9	122.6	122.6	122.5
∠HCC	121.7	119.7	115.6	114.8	114.8	115.3	115.4
∠CCN		178.2	178.7	177.8	178.0	177.5	178.3
μ (D)	3.92 ± 0.07[c]		4.05	0.0028	3.90	3.80	0.1532
ΔE				−12.65	−24.46	−16.68	−31.12
MP2 ΔE				−17.53	−31.86	−21.62	−38.64

[a] Reference 92. [b] Reference 58. [c] Reference 93. [d] Lengths (pm) and angles (deg) in trimers I and II are those corresponding to the central molecule.

the central antiparallel monomer, which lies in a different plane. Very close trimer structures have been recently reported by Katayama et al.[59] in acetonitrile, propionitrile, acrylonitrile, and benzonitrile in the liquid-phase using X-ray diffraction with CCD detection. Table 5 shows the calculated bond lengths and angles for the acrylonitrile molecule in both isolated form and as part of the different oligomers (dimer and trimers I−III) considered here. Experimental data from gaseous state[58,92] indicate that optimized monomer structure does not differ by more than ±1% in the principal bond lengths (C═C, C−C, and C≡N). The calculated C−H bond lengths are not comparable with experimental data because in both studies, only the averaged C−H distances are given. Furthermore, these seem to be overestimated in earlier work.[58] The main discrepancy arises from the C═CH angle that is systematically underestimated for all the studied conformations. One interesting conclusion that can be obtained from the data presented in Table 5 is that monomer geometry does not change substantially when it is part of a more complex supramolecular structure (dimer or trimer). This observation, in complete agreement with those

TABLE 6: Optimized Intermolecular Distances and Angles in Acrylonitrile Dimer and Trimers at the B3LYP/6-311++G Level of Theory[a]**

dimer		trimer I		trimer II		trimer III	
parameter	value	parameter	value	parameter	value	parameter	value
$C_3\cdots C_{10}$	348.0	$C_3\cdots C_{10}$	351.2	$C_3\cdots C_{10}$	550.0	$C_3\cdots C_{10}$	466.5
$N_4\cdots H_{14}$	265.4	$C_3\cdots C_{17}$	405.3	$C_3\cdots C_{17}$	358.3	$C_3\cdots C_{17}$	466.9
$N_{11}\cdots H_7$	265.4	$N_4\cdots H_{14}$	266.9	$N_4\cdots H_{21}$	326.9	$N_4\cdots H_{21}$	237.4
$\angle C_3N_4H_{14}$	115.7	$N_4\cdots H_{20}$	248.5	$N_{11}\cdots H_{21}$	326.6	$N_{11}\cdots H_7$	237.5
$\angle C_{10}N_{11}H_7$	115.7	$N_{11}\cdots H_7$	268.1	$N_{18}\cdots H_7$	263.1	$N_{18}\cdots H_{14}$	237.4
$\angle C_3N_4C_{10}$	78.6	$N_{18}\cdots H_6$	247.8	$N_{18}\cdots H_{14}$	263.3		
		$\angle C_3N_4H_{14}$	114.5	$\angle C_3N_4H_{21}$	109.5	$\angle C_3N_4H_{21}$	143.3
		$\angle C_3N_4H_{20}$	131.2	$\angle C_{10}N_{11}H_{21}$	109.6	$\angle C_{10}N_{11}H_7$	142.9
		$\angle C_{10}N_{11}H_7$	114.4	$\angle C_{17}N_{18}H_7$	114.4	$\angle C_{17}N_{18}H_{14}$	142.9
		$\angle C_{17}N_{18}H_6$	132.4	$\angle C_{17}N_{18}H_{14}$	114.5		
		$\angle C_3N_4C_{10}$	78.0	$\angle C_3N_4C_{10}$	80.5		
		$\angle C_3N_4C_{17}$	77.2	$\angle C_3N_4C_{17}$	75.8		

[a] Lengths are in pm and angles are in degrees. Atomic subindexes are those of Figure 7.

TABLE 7: Calculated Vibrational Wavenumbers (cm^{-1}) for Acrylonitrile at the B3LYP/6-311++G Level of Theory and Percentage Differences with the Experimental IR Gas-Phase Spectra[c]**

normal mode	symmetry	calculated	observed[a,b]	difference (%)	approximate description
ν_1	A′	3245	3125	3.8	(C−H) asym. stretching of XH_2
ν_2		3169	3078	3.0	(C−H) stretching of C−H
ν_3		3152	3042	3.6	(C−H) sym. stretching of CH_2
ν_4		2333	2239	4.2	(C≡N) stretching
ν_5		1672	1615	3.5	(C═C) stretching
ν_6		1445	1416	2.0	(CH_2) deformation
ν_7		1319	1282	2.9	(C−H) rocking
ν_8		1110	1096	1.3	(CH_2) rocking
ν_9		882	869	1.5	(C−C) stretching
ν_{10}		582	N.O.		(C═C−C) bending
ν_{11}		239	229	4.3	in-plane (C−C≡N) bending
ν_{12}	A″	1005	972	3.4	(C−H) wagging
ν_{13}		990	954	3.8	(CH_2) wagging
ν_{14}		712	683	4.3	(C═C) torsion
ν_{15}		350	333	5.0	out-of-plane (C−C≡N) bending

[a] Reference 40. [b] Reference 102. [c] N.O. = not observed.

previously reported for acetonitrile,[13,23,24,26,91] suggests that the intramolecular interactions present in acrylonitrile oligomers are of a nondirectional nature.

The calculated dipole moments are very close to the experimental value observed for the monomer, except for the centrosymmetric dimer and trimer (trimer III). They raise again the controversial question (see ref 62 and references therein) of the formation of dimers or higher centrosymmetric aggregates in nitriles. Indeed, it is difficult to understand how acrylonitrile, a liquid of moderately high dielectric constant ($\epsilon = 33.0$),[93] could permit an equilibrium between two different molecular forms, one of which has a dipole moment near zero. The same question applies to other nitriles with higher dielectric constants (e.g., acetonitrile) where the centrosymmetric dimer form has no dipole moment.

BSSE-corrected energy minima corresponding to the different acrylonitrile oligomers indicate that the cyclic trimer (trimer III) seems to be the most stable structure, although dimer is also more stable than trimers I and II if we consider the interaction energy per molecule. These results are consistent with those reported for acetonitrile.[21,23] To have a better knowledge about the interaction energies, MP2 optimizations were undertaken for all the acrylonitrile oligomers. As can be observed in Table 5, MP2 energies are consistently larger than those calculated using DFT but the general picture does not change and the relative order is the same in both series of calculations.

Table 6 summarizes intermolecular distances and angles in the oligomers of interest. The closest approach between monomers is the distance between two antiparallel C≡N bonds ($C_3\cdots C_{10}$ distance) and lies in the range 348−358 pm. This figure agrees very well with those obtained for acetonitrile dimers using various theoretical levels,[23,24,91] all of which are close to 350 pm. On the other hand, N···H distances range from 237 to 327 pm, with C≡N···H angles far from linearity. This implies that the presence of hydrogen bonds must be discarded, as was previously discussed in the Raman spectroscopy section. Furthermore, if any significant H-bonding would contribute to the stabilization of the oligomer structure, then the calculated C_2−H bond distances should increase from the corresponding one of the monomer. Likewise, as previously reported,[63] C≡N bond lengths should decrease. As shown in Table 2, no such findings are made.

Table 7 gives the predicted vibrational spectrum for acrylonitrile in the gaseous state. The average error of the wavenumbers is $3.33 \pm 1.10\%$, which further supports the ability of DFT/B3LYP combined with the 6-311++G** basis set to calculate well-fitted vibrational spectra.[94−99] In addition to the near absence of geometrical changes when the monomer oligomerizes, the calculated vibrational spectra from dimer and trimers (Table 8) are very close to that obtained for the monomer with two main exceptions: the fundamentals with participation of the nitrile group (ν_4, ν_{11}, ν_{15}) and C−H wagging mode (ν_{12}). As the changes corresponding to the C≡N stretching vibration (ν_4) are quite small, we recalculate the results (structure and spectra) corresponding to the dimer but correcting for BSSE. The BSSE-corrected frequencies are 2328.1 and 2328.2 cm^{-1},

TABLE 8: Calculated Vibrational Wavenumbers (cm^{-1}) for Gas-Phase Acrylonitrile Species at the B3LYP/6-311++G Level of Theory**

normal mode	monomer	dimer[a]	trimer I[b]	trimer II[b]	trimer III[c]
ν_1	3245	3243	3240	3245	3241
ν_2	3169	3170	3170	3186	3156
ν_3	3152	3151	3142	3152	3149
ν_4	2333	2328	2322	2329	2328
ν_5	1672	1673	1668	1673	1672
ν_6	1445	1445	1452	1444	1447
ν_7	1319	1318	1321	1321	1332
ν_8	1110	1114	1119	1112	1117
ν_9	882	881	883	882	881
ν_{10}	582	582	590	586	587
ν_{11}	239	241	251	244	246
ν_{12}	1005	1022	1031	1000	1040
ν_{13}	990	989	1019	989	992
ν_{14}	712	719	722	713	724
ν_{15}	350	358	372	357	365

[a] Mean of the two fundamentals arising from both monomers. [b] Data from the central acrylonitrile monomer. [c] Mean of the three monomers.

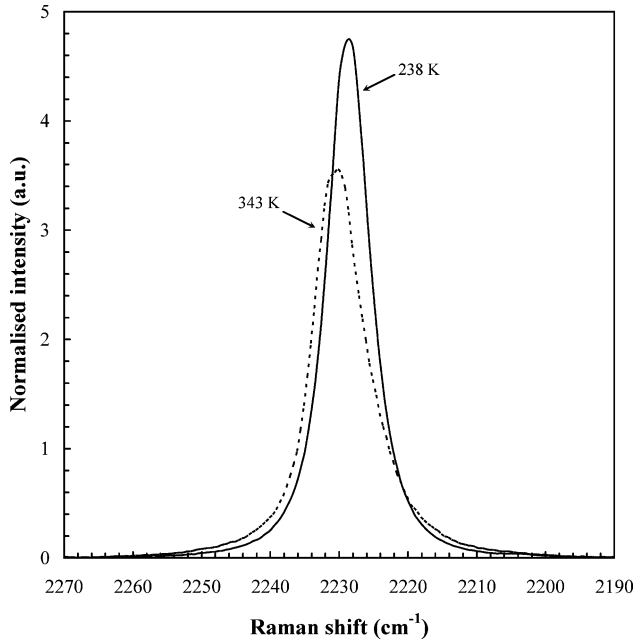

Figure 8. ν(C≡N) Raman spectral region of acrylonitrile at two different temperatures.

virtually identical to those previously obtained. These results are qualitatively fitted with the reported spectral changes if the acrylonitrile in CCl_4 dilution process has a change from oligomeric to monomeric forms. Indeed, ab initio computations predict that all normal modes with the exception of ν_4 must move toward lower wavenumbers in going from self-associated to free acrylonitrile. This result is consistent with previous ab initio computations[17] and it is exactly what we have found experimentally by dissolving acrylonitrile in CCl_4 (see Figure 2). Furthermore, the prediction that the ν(C≡N) band must shift toward lower wavenumbers between -5 and -11 cm^{-1} (dimer and trimer I, respectively) is in quantitative agreement with the band-fitting results. Another important point is the predicted change in the Raman (and infrared) band intensities. The computations predict important changes in the IR intensities, always increasing from monomer to self-associated species. This is in qualitative agreement with previous results[10,13,16,100] which report significant decreases in the IR molar absorption coefficients when nitriles are dissolved in nonpolar aprotic solvents.

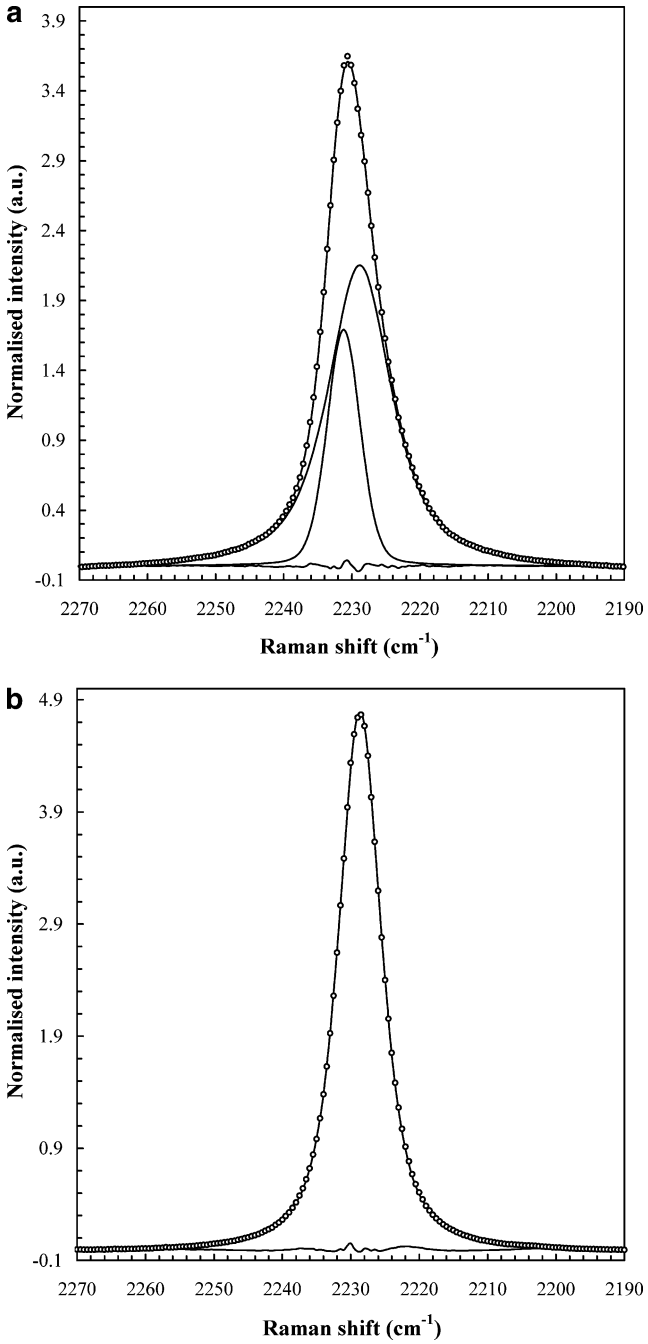

Figure 9. Results (experimental spectrum, fitted spectrum, components, and residual) of the band-fitting procedure in the ν(C≡N) complex band. (a) Neat acrylonitrile at 343 K. (b) Neat acrylonitrile at 238 K. In the lower temperature, only one component is needed to fit the experimental data. Points: experimental spectrum.

On the other hand, the effect of self-association over the IR molar absorption coefficients also explains the observed increase in the ν(C≡N) IR band intensity from the vapor to the liquid state.[10,101] Calculated changes in the Raman intensities are more informative and allow one to discard the planar trimer (trimer I) as a possible structure in the liquid state. This is because the Raman intensity should decrease in the self-associated species, while experimental data demonstrate the opposite. Our experimentally calculated molar Raman scattering factors (J) demonstrate an intensity increase of approximately 56% from the monomer to oligomer ν(C≡N) band. This is approximately an average of the calculated values for dimer and trimer II. To decide between these two structures for self-associated acry-

TABLE 9: Band-Fitting Results in the C≡N Stretching Raman Band Contour of Acrylonitrile at Different Temperatures[a]

	monomer			trimer		
T (K)	center	fwhh	Lorentz (%)	center	fwhh	Lorentz (%)
343	2231.3	5.76	18.7	2229.0	11.24	75.2
328	2230.8	5.12	19.4	2228.7	10.76	68.6
313	2230.7	5.16	17.9	2228.9	10.17	67.7
298	2230.2	5.12	21.4	2228.7	10.35	64.0
283	2230.0	5.03	20.8	2228.6	10.19	70.4
238				2228.5	7.41	67.2

[a] Units: center and full width at half-height (fwhh), cm^{-1}.

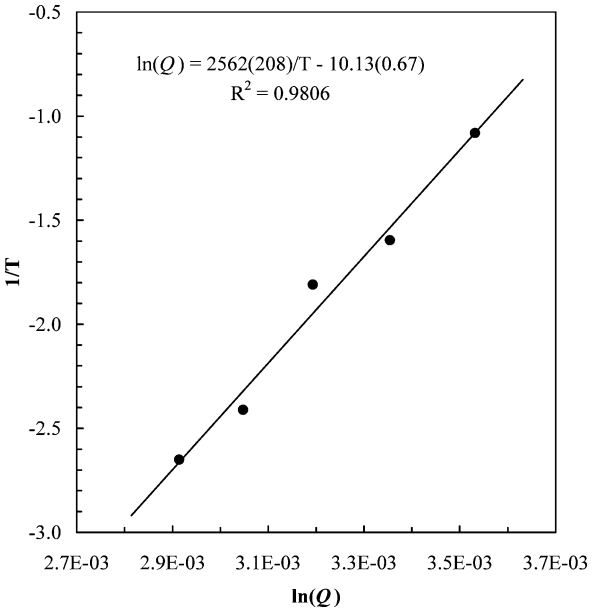

Figure 10. Arrhenius' plot for the calculated equilibrium constants assuming the stoichiometry 3 monomer ⇄ trimer. In brackets, standard errors.

lonitrile in the liquid phase, other factors must be considered. Dannhauser and Flueckinger[1] discussed the dipole moment of the centrosymmetric dimer, which is very close to zero, and the contradiction of an apolar structure in a quite polar liquid. In our opinion, acrylonitrile self-associates through a structure similar to trimer II. In addition to the reported X-ray diffraction structure of liquid acrylonitrile,[59] which fully supports this conclusion, very stable acrylonitrile trimers have been identified as anions (i.e., solvating one electron) by mass spectrometry.[9] Also, we have experimentally obtained a solvation number of three for lithium ion dissolved in acrylonitrile with different counteranions such as triflate,[44] perchlorate,[42] and tetrafluoroborate.[49]

3.3. Acryonitrile Raman Spectra at Different Temperatures. The main reason that Loewenschuss and Yellin[34] argued in favor of discarding the chemical equilibrium between monomer and higher aggregates in liquid acetonitrile was the apparent absence of noticeable changes in the C≡N stretching Raman band shape or position because of temperature changes. As Figure 8 demonstrates, the situation in acrylonitrile is rather different. At 238 K, the ν(C≡N) Raman band in acrylonitrile has a very symmetric shape that becomes asymmetric toward the lower wavenumbers and slightly upshifts when the temperature is increased to 343 K. Thus, the effect of the temperature over the structure of the liquid seems to be parallel to that observed with the dilution in CCl_4: increasing temperature and increasing dilution both raise the presence of the monomeric form. Furthermore, such behavior is as expected for an exothermic equilibrium, in agreement with the ab initio computations (see Table 5) and previous experimental macroscopic results.[1,4] PCA carried out for Raman spectra at eight different temperatures from 238 to 343 K in steps of 15 K gives the same result obtained previously from changing the acrylonitrile concentration in CCl_4. The disturbing factor (temperature) promotes the presence of the component located at higher wavenumbers (monomer). The corresponding band-fitting procedure is shown in Figure 9. Table 9 gives the corresponding numerical results. For the lowest temperature studied, the C≡N stretching Raman band becomes completely symmetric, thus requiring only one component for the fit. Taking into account the temperature range over which acrylonitrile remains in liquid state (from 189.7 to 350.5 K),[93] the thermodynamic stability of the self-associated species is evident. Close to the boiling point (343 K), the mole fraction of the trimer was 0.65. After the intensity ratios of both components have been obtained from the band-fitting procedure, the corresponding concentrations can be computed using the previously calculated Raman molar intensity coefficients. From eq 8

$$C_T \frac{J_A}{I_A} - \frac{J_A}{J_F}\frac{I_F}{I_A} = 1 \tag{9}$$

but

$$\frac{J_A}{I_A} = C_A \tag{10}$$

Substituting in eq 9

$$\frac{C_T}{C_A} = 1 + \frac{J_A}{J_F}\frac{I_F}{I_A} \tag{11}$$

Then, the concentration quotients

$$Q = \frac{[\text{trimer}]}{[\text{monomer}]^3} \tag{12}$$

are immediately obtained at the different temperatures. The Arrhenius plot is given in Figure 10. Only the spectra of the five higher temperatures were computed because of the very low concentration of monomer in the samples at 268 and 253 K. From the fitted line, $\Delta H_{association} = -22 \pm 2$ kJ·mol^{-1}. This result agrees fairly well with that obtained from ab initio calculations for the gas-phase equilibrium ($\Delta H_{association} = -13.70$ kJ·mol^{-1}), further demonstrating the thermodynamic stability of the self-associated species.

4. Conclusions

Liquid structure of acrylonitrile can be described as an equilibrium between monomers and higher aggregates. These are probably nonplanar trimers whose structure is maintained through dipole−dipole interactions rather than by hydrogen bonding. At ambient temperature, the composition of acrylonitrile is 25% monomers and 75% trimers. Close to the boiling point, trimers still represent 65% of the liquid composition. The self-association equilibrium is sensitive to both changes in concentration and temperature. Progressive dilution in CCl_4 and increasing temperature promote the presence of monomeric acrylonitrile. On the other hand, only the associated species can be observed at 238 K.

The obtained experimental results agree both qualitatively and quantitatively with those computed ab initio at the B3LYP/6-311++G** theoretical level. The enthalpy of association has been estimated as -22 ± 2 kJ·mol^{-1}, which indicates that the acrylonitrile trimer form is a stable chemical entity.

Acknowledgment. Funded by Spanish Ministerio de Educación y Ciencia; Grant Number PR2006-0104.

References and Notes

(1) Dannhauser, W.; Flueckinger, A. F. *J. Phys. Chem.* **1964**, *68*, 1814.
(2) Buckinham, A. D.; Raab, R. E. *J. Chem. Soc.* **1961**, 5511.
(3) Haijun, W.; Guokang, Z.; Mingzhi, C. *J. Chem. Thermodyn.* **1993**, *25*, 949.
(4) Saum, A. M. *J. Polym. Sci.* **1960**, *42*, 57.
(5) Jackowski, K.; Wielogórska, E. *J. Mol. Struct.* **1995**, *355*, 287.
(6) Jackowski, K. *Chem. Phys. Lett.* **1992**, *194*, 167.
(7) Saito, H.; Tanaka, Y.; Nagata, S.; Nukada, K. *Can. J. Chem.* **1973**, *51*, 2118.
(8) Olesik, S. V.; Taylor, J. W. *Int. J. Mass Spectrom. Ion Processes* **1984**, *57*, 299.
(9) Tsukuda, T.; Kondow, T. *J. Chem. Phys.* **1991**, *95*, 6989.
(10) Thomas, B. H.; Orville-Thomas, W. J. *J. Mol. Struct.* **1971**, *7*, 123.
(11) Knözinger, E.; Leutloff, D. *J. Chem. Phys.* **1981**, *74*, 4812.
(12) Inaba, R.; Okamoto, H.; Yoshihara, K.; Tasumi, M. *J. Phys. Chem.* **1992**, *96*, 8385.
(13) Mathieu, D.; Defranceschi, M.; Delhalle, J. *Int. J. Quantum Chem.* **1993**, *45*, 735.
(14) Deiseroth, H. J.; Popp, S.; Kollhoff, H.; Langel, W.; Kngzinger, E. *J. Mol. Struct.* **1988**, *174*, 89.
(15) Asthana, B. P.; Deckert, V.; Shukla, M. K.; Kiefer, W. *Chem. Phys. Lett.* **2000**, *326*, 123.
(16) Cha, J. N.; Cheong, B. S.; Cho, H. G. *J. Mol. Struct.* **2001**, *570*, 97.
(17) Tukhvatullin, F. H.; Jumabaev, A.; Muradov, G.; Hushvaktov, H. A.; Absanov, A. A. *J. Raman Spectrosc.* **2005**, *36*, 932.
(18) Srivastava, S. K.; Ojha, A. K.; Sinha, P. K.; Asthana, B. P.; Singh, R. *J. Raman Spectrosc.* **2006**, *37*, 68.
(19) Mathieu, D.; Defranceschi, M.; Lecayon, G.; Delhalle, J. *C. R. Acad. Sci. II* **1992**, *315*, 1181.
(20) Dessent, C. E. H.; Kim, J.; Johnson, M. A. *J. Phys. Chem.* **1996**, *100*, 12.
(21) Cabaleiro-Lago, E. M.; Ríos, M. A. *J. Phys. Chem. A* **1997**, *101*, 8327.
(22) Siebers, J. G.; Buck, U.; Beu, T. A. *Chem. Phys.* **1998**, *239*, 549.
(23) Cabaleiro-Lago, E. M.; Hermida Ramón, J. M.; Peña Gallego, A.; Martínez Núñez, A.; Fernández Ramos, A. *J. Mol. Struct. (THEOCHEM)* **2000**, *498*, 21.
(24) Ford, T. A.; Glasser, L. *Int. J. Quantum Chem.* **2001**, *84*, 226.
(25) Okuno, Y.; Yokoyama, T.; Yokoyama, S.; Kamikado, T.; Mashiko, S. *J. Am. Chem. Soc.* **2002**, *124*, 7218.
(26) Mata, R. A.; Costa, Cabral, B. J. *J. Mol. Struct. (THEOCHEM)* **2004**, *673*, 155.
(27) Takayanagi, T. *J. Chem. Phys.* **2005**, *122*, Art. No. 244307.
(28) Fawcett, W. R.; Liu, G.; Kessler, T. E. *J. Phys. Chem.* **1993**, *97*, 9293.
(29) Stoev, M.; Makarov, A.; Alía, J. M. *Spectrosc. Lett.* **1995**, *28*, 1251.
(30) Tanabe, K. *Chem. Phys.* **1981**, *63*, 135.
(31) Abramczyk, H. *Chem. Phys. Lett.* **1983**, *100*, 287.
(32) Bhattacharjee, D.; Ghosh, A.; Misra, T. N.; Nandy, S. K. *J. Raman Spectrosc.* **1996**, *27*, 457.
(33) Griffiths, J. E. *J. Chem. Phys.* **1973**, *59*, 751.
(34) Loewenschuss, A.; Yellin, N. *Spectrochim. Acta, Part A* **1975**, *31*, 207.
(35) Fernández-Bertrán, J.; La Serna, B.; Doerffel, K.; Dathe, K.; Kabisch, G. *J. Mol. Struct.* **1982**, *95*, 1.
(36) McKean, D. C.; Machray, S. *Spectrochim. Acta, Part A* **1988**, *44*, 533.
(37) Hashimoto, S.; Ohba, T.; Ikawa, S. *Chem. Phys.* **1989**, *138*, 63.
(38) Stolov, A. A.; Morozov, A. I.; Remizov, A. B. *Spectrochim. Acta, Part A* **2000**, *56*, 485.
(39) Suzuki, I.; Nakagawa, J.; Fujiyama, T. *Spectrochim. Acta, Part A* **1977**, *33*, 689.
(40) Halverson, F.; Stamm, R. F.; Whalen, J. J. *J. Chem. Phys.* **1948**, *16*, 808.
(41) Alía, J. M.; Edwards, H. G. M. *J. Mol. Struct.* **1995**, *354*, 97.
(42) Alía, J. J.; Edwards, H. G. M.; Moore, J. *J. Raman Spectrosc.* **1995**, *26*, 715.
(43) Alía, J. M.; Edwards, H. G. M.; Moore, J. *Spectrochim. Acta, Part A* **1995**, *51*, 2039.
(44) Alía, J. M.; Díaz de Mera, Y.; Edwards, H. G. M.; García, F. J.; Lawson, E. E. *Z. Phys. Chem. (Munich)* **1996**, *196*, 209.
(45) Alía, J. M.; Edwards, H. G. M.; Moore, J. *J. Chem. Soc., Faraday Trans.* **1996**, *92*, 1187.
(46) Alía, J. M.; Edwards, H. G. M.; Moore, J. *Spectrochim. Acta, Part A* **1996**, *52*, 1403.
(47) Alía, J. M.; Edwards, H. G. M.; Díaz de Mera, Y.; Lawson, E. E. *J. Solution Chem.* **1997**, *28*, 69.
(48) Alía, J. M.; Edwards, H. G. M.; Moore, J. *Mikrochim. Acta* **1997**, *14*, 733.
(49) Alía, J. M.; Edwards, H. G. M. *J. Solution Chem.* **2000**, *29*, 781.
(50) Alía, J. M.; Edwards, H. G. M.; García, F. J.; Lawson, E. E. *J. Mol. Struct.* **2001**, *43*, 565−566.
(51) Alía, J. M.; Edwards, H. G. M.; Kiernan, B. M. *Spectrochim. Acta, Part A* **2005**, *61*, 2939.
(52) Bryan, S. J.; Hugget, P. G.; Wade, K.; Daniels, J. A.; Jennings, J. R. *Coord. Chem. Rev.* **1982**, *44*, 149.
(53) Raghuvansh, P.; Srivastava, S. K.; Singh, R. K.; Asthana, B. P.; Kiefer, W. *Phys. Chem. Chem. Phys.* **2004**, *6*, 531.
(54) Singh, R. K.; Asthana, B. P.; Singh, P. R.; Chakraborty, T.; Verma, A. L. *J. Raman Spectrosc.* **1998**, *29*, 561.
(55) Pemberton, R. S.; Shurvell, H. F. *J. Raman Spectrosc.* **1995**, *26*, 373.
(56) Quadri, S. M.; Shurvell, H. F. *Spectrochim. Acta, Part A* **1995**, *51*, 1355.
(57) Girling, R. B.; Shurvell, H. F. *Vib. Spectrosc.* **1998**, *18*, 77.
(58) Fukuyama, T.; Kuchitsu, K. *J. Mol. Struct.* **1970**, *5*, 131.
(59) Katayama, M.; Komori, K.; Ozutsumi, K.; Ohtaki, H. *Z. Phys. Chem. (Munich)* **2004**, *218*, 659.
(60) Becke, A. D. *Phys. Rev. A* **1988**, *38*, 3098.
(61) Lee, C.; Yang, W.; Parr, R. G. *Phys. Rev. B* **1988**, *37*, 785.
(62) Becke, A. D. *J. Chem. Phys.* **1993**, *98*, 5648.
(63) Alía, J. M.; Edwards, H. G. M. *J. Phys. Chem. A* **2005**, *109*, 7977.
(64) Alcolea Palafox, M.; Rastogui, V. K.; Mittal, L. *Int. J. Quantum Chem.* **2003**, *94*, 189.
(65) Wu, D. Y.; Ren, B.; Jiang, Y. X.; Xu, X.; Tian, Z. Q. *J. Phys. Chem. A* **2002**, *106*, 9042.
(66) Johnson, B. G.; Gill, P. W.; Pople, J. A. *J. Chem. Phys.* **1993**, *98*, 5612.
(67) Simon, S.; Duran, M.; Dannemberg, J. J. *J. Chem. Phys.* **1996**, *105*, 11024.
(68) Boys, S. F.; Bernardi, F. *Mol. Phys.* **1970**, *19*, 553.
(69) Frisch, M. J.; Trucks, G. W.; Schlegel, H. B.; Scuseria, G. E.; Robb, M. A.; Cheeseman, J. R.; Montgomery, J. A., Jr.; Vreven, T.; Kudin, K. N.; Burant, J. C.; Millam, J. M.; Iyengar, S. S.; Tomasi, J.; Barone, V.; Mennucci, B.; Cossi, M.; Scalmani, G.; Rega, N.; Petersson, G. A.; Nakatsuji, H.; Hada, M.; Ehara, M.; Toyota, K.; Fukuda, R.; Hasegawa, J.; Ishida, M.; Nakajima, T.; Honda, Y.; Kitao, O.; Nakai, H.; Klene, M.; Li, X.; Knox, J. E.; Hratchian, H. P.; Cross, J. B.; Bakken, V.; Adamo, C.; Jaramillo, J.; Gomperts, R.; Stratmann, R. E.; Yazyev, O.; Austin, A. J.; Cammi, R.; Pomelli, C.; Ochterski, J. W.; Ayala, P. Y.; Morokuma, K.; Voth, G. A.; Salvador, P.; Dannenberg, J. J.; Zakrzewski, V. G.; Dapprich, S.; Daniels, A. D.; Strain, M. C.; Farkas, O.; Malick, D. K.; Rabuck, A. D.; Raghavachari, K.; Foresman, J. B.; Ortiz, J. V.; Cui, Q.; Baboul, A. G.; Clifford, S.; Cioslowski, J.; Stefanov, B. B.; Liu, G.; Liashenko, A.; Piskorz, P.; Komaromi, I.; Martin, R. L.; Fox, D. J.; Keith, T.; Al-Laham, M. A.; Peng, C. Y.; Nanayakkara, A.; Challacombe, M.; Gill, P. M. W.; Johnson, B.; Chen, W.; Wong, M. W.; Gonzalez, C.; Pople, J. A. *Gaussian 03*, Revision C.02; Gaussian, Inc.: Wallingford, CT, 2004.
(70) Semichem Inc., P.O. Box 1649, Shawnee Mission, KS, Institutional License, UCLM.
(71) Statistical Graphics Corp., Institutional License, UCLM.
(72) Max, J. J.; Chapados, C. *J. Chem. Phys.* **2005**, *112*, 14504.
(73) Zhou, Z.; Shi, Y.; Zhou, X. *J. Phys. Chem. A* **2004**, *108*, 813.
(74) Kollman, P.; Allen, A. *Chem. Rev.* **1972**, *72*, 283.
(75) Hobza, P.; Havlas, Z. *Chem. Rev.* **2000**, *100*, 4253.
(76) Thomas, B. H.; Orville-Thomas, W. J. *J. Mol. Struct.* **1969**, *3*, 191.
(77) Bernstein, M. P.; Sandford, S. A.; Allamandola, L. J. *Astrophys. J.* **1997**, *476*, 932.
(78) Barthel, J.; Deser, R. *J. Mol. Liq.* **1995**, *67*, 95.
(79) Loring, J. S.; Fawcett, W. R. *J. Phys. Chem. A* **1999**, *103*, 3608.
(80) Perelygin, I. S.; Krauze, A. S.; Itkulov, I. G.; Makkamboev, D. *Zh. Fiz. Khim.* **1992**, *66*, 2965.
(81) Malinowski, E. R. *Factor Analysis in Chemistry*, 2nd ed.; John Wiley & Sons, Inc.: New York, 1991.
(82) Shurvell, H. F.; Bulmer, J. T. In *Vibrational Spectra and Structure*; Durig, J. R., Ed.; Elsevier Scientific Publishing Company: Amsterdam, 1977; p 91.
(83) Irish, D. E.; Ozeki, T. In *Analytical Raman Spectroscopy*; Graselli, J., Bulkin, B. J., Eds.; John Wiley & Sons, Inc.: New York, 1991; p 59.
(84) van Heumen, J.; Ozeki, T.; Irish, D. E. *Can. J. Chem.* **1989**, *67*, 2030.

(85) Bentham, P. B.; Romak, G. C.; Shurvell, H. F. *Can. J. Chem.* **1985**, *63*, 2303.
(86) Lalic, M.; Sasic, S.; Antic-Jovanovic, A.; Jeremic, M. *Spectrosc. Lett.* **1998**, *31*, 335.
(87) Sasic, S.; Kuzmanovic, M. *J. Raman Spectrosc.* **1998**, *29*, 593.
(88) Cabaço, M. I.; Besnard, M.; Yarwood, J. *Mol. Phys.* **1992**, *75*, 139.
(89) Alía, J. M.; Edwards, H. G. M.; Kiernan, B. M. *J. Raman Spectrosc.* **2004**, *35*, 111.
(90) Alía, J. M.; Edwards, H. G. M.; Kiernan, B. M. *Spectrochim. Acta, Part A* **2004**, *60*, 1533.
(91) Pacansky, J. *J. Phys. Chem.* **1977**, *81*, 2240.
(92) Gerry, M. C. L.; Yamada, K.; Winnewisser, G. *J. Phys. Chem. Ref. Data* **1979**, *8*, 107.
(93) *Handbook of Chemistry and Physics*; Lide, D. R., Ed.; CRC Press: Boca Raton, FL, 2006−2007.
(94) Rivail, J. L.; Rinaldi, D.; Dillet, V. *Mol. Phys.* **1996**, *89*, 1521.
(95) Coussan, S.; Bouteiller, Y.; Perchard, J. P.; Brenner, V.; Millié, P.; Zheng, W. Q.; Talbot, F. *J. Chem. Phys.* **1999**, *110*, 10046.
(96) Bakó, I.; Megyes, T.; Pálinkás, G. *Chem. Phys.* **2005**, *316*, 235.
(97) Giesen, D. J.; Phillips, J. A. *J. Phys. Chem. A* **2003**, *107*, 4009.
(98) Burneau, A.; Génin, F.; Quilés, F. *Phys. Chem. Chem. Phys.* **2000**, *2*, 5020.
(99) Barone, V. *J. Phys. Chem. A* **2004**, *108*, 4146.
(100) Foffani, A.; Pecile, C.; Pietra, F. *Nuovo Cimento Soc. Ital. Fis.* **1959**, *13*, 213.
(101) Jesson, J. P.; Thompson, H. W. *Spectrochim. Acta* **1958**, *13*, 217.
(102) Cole, A. R. H.; Green, A. A. *J. Mol. Spectrosc.* **1973**, *48*, 246.